Global Analysis of the Acid-Induced and Urea-Induced Unfolding of Staphylococcal Nuclease and Two of Its Variants†

Roxana M. Ionescu and Maurice R. Eftink*

Department of Chemistry, University of Mississippi, University, Mississippi 38677

Received April 22, 1996; Revised Manuscript Received November 19, 1996⊗

ABSTRACT: We have studied the equilibrium unfolding of staphylococcal nuclease and two of its variants, V66W and V66W′, over two perturbation axes (acid-induced unfolding as a function of urea concentration and urea-induced unfolding as a function of pH). The transitions were monitored by simultaneous measurements of circular dichroism and fluorescence. With this multidimensional array of data (2 perturbation axes and 2 signals), we present a strategy of performing a global analysis, over as many as 12 individual data sets, to test various models for the unfolding process, to determine with greater confidence the pertinent thermodynamic parameters, and to characterize unfolding intermediates. For example, wild-type nuclease shows a cooperative two-state transition with either urea or pH as denaturant, but the global fits are improved when the model is expanded to include a pH dependence of the urea *m* value or when two distinct classes of protonic groups are considered. The best fit for wild-type nuclease is with $\Delta G°_{0,UN}$ = 6.4 kcal/mol at pH 7, with the acid-induced unfolding being triggered by protonation of three to five carboxylate groups (with possible contribution from His^{121}), and with the urea m = 2.5 kcal mol^{-1} M^{-1}. V66W′ lacks the last 13 amino acids on the C-terminus, has a tryptophan at position 66, has a predominantly β-sheet structure, and is less stable than the wild type. For V66W′, $\Delta G°_{0,UN}$ = 1.6 kcal/mol, m = 1.2 kcal mol^{-1} M^{-1}, and there are two or three groups responsible for acid unfolding. V66W, a full-length mutant with two tryptophan residues, unfolds via a three-state mechanism: native ⇌ intermediate ⇌ unfolded. It appears that its β-barrel subdomain retains structure in the intermediate state. Assuming that the unfolding of V66W′ and the β-barrel subdomain of V66W can be described by the same thermodynamic parameters, a global analysis enabled a description of the α subdomain of V66W with $\Delta G°_{0,IN}$ = 2.7 kcal/mol, m_{IN} = 1.1 kcal mol^{-1} M^{-1}, and with the acid unfolding being triggered by protonation of a single group. This group has a pK_a around 6 in the unfolded state, suggesting that the state of protonation of a histidine residue may contribute significantly to the stability of V66W.

We have studied the dependence of the free energy of unfolding for staphylococcal nuclease on both pH and urea concentration. Theoretical models have been developed to predict a protein's stability as a function of pH (Tanford, 1970; Alonso et al., 1991; Yang & Honig, 1994) or as a function of urea concentration (Tanford, 1970; Schellman, 1978). Previous studies (Pace et al., 1990, 1992; Yao & Bolen, 1995), which have involved both urea and acid as denaturants, have not attempted to fit all of the data to a composite thermodynamic model. One study which considered a simultaneous analysis of pH- and urea-induced unfolding was that of Barrick and Baldwin (1993) on the stability of apomyoglobin. In the work presented here, we have globally analyzed circular dichroism (CD)[1] and fluorescence data (which were simultaneously recorded for the same protein sample), and we have used a more flexible model than that previously used by Barrick and Baldwin (1993). The "global analysis" represents a concomitant analysis of multiple data sets; in our case, 12 data sets were considered for each protein.

Wild-type staphylococcal nuclease A (WT SNase) is a small protein of 149 residues, having a secondary structure composed of 3 α-helices and 5 β-sheet strands. There is only one tryptophan residue at position 140, which is near the end of the last and longest α-helical segment in the protein. The α-helix regions (residues 32−70 and 99−141) and the β-barrel part (residues 1−31 and 71−98) form two subdomains which unfold in a cooperative way (Xie et al., 1994). If the coupling between the domains is perturbed or if the β-barrel is stabilized by mutations, it has been shown that the unfolding can deviate from a two-state process (Carra et al., 1994c).

In the studies presented below, we find that the acid- and-urea induced unfolding of WT, at low ionic strength and 20 °C, can be described by a two-state process. The same conclusion is reached for the case of V66W′, a variant of WT SNase that contains only residues 1−136 and has a single tryptophan residue at position 66 (instead of valine).

The full-length mutant V66W, with tryptophans at positions 66 and 140, contains a fluorescent residue in each subdomain. This mutant clearly shows a deviation from a two-state process, when unfolded by temperature or guanidine hydrochloride (Gittis et al., 1993; Carra et al., 1994c). As will be shown, an intermediate state becomes significantly populated during pH- and urea-induced unfolding of this protein, as reflected in both CD and fluorescence data. We have performed a global analysis for V66W by considering

† This research was supported by NSF Grant MCB 9407167.

* To whom correspondence should be addressed.

⊗ Abstract published in *Advance ACS Abstracts,* January 1, 1997.

[1] Abbreviations: CD, circular dichroism; GuHCl, guanidine hydrochloride; SNase, staphylococcal nuclease; V66W, SNase mutant that has tryptophan at position 66 instead of valine; V66W′, fragment of V66W containing only residues 1−136; WT, wild type.

S0006-2960(96)00968-3 CCC: $14.00

the unfolding to occur as a succession of two first-order phase transitions, corresponding to the unfolding of the α and β subdomains, respectively. A very good fit to the data was obtained when the second transition (corresponding to the β-barrel unfolding) was assumed to be described by the same thermodynamic parameters as those found for the unfolding of V66W′.

MATERIALS AND METHODS

Materials

Plasmids (kindly supplied by Dr. Wesley Stites, University of Arkansas) containing the genes of the WT, V66W, and V66W′ variants of SNase were expressed in *E. coli*, following the protocol described by Shortle and Meeker (1989). The purity of the proteins produced was found by denaturing electrophoresis to be higher than 95%. Protein concentration was determined using molar extinction coefficients at 280 nm of 15 600 M^{-1} cm^{-1} for WT and V66W′, and 21 100 M^{-1} cm^{-1} for V66W. The samples were prepared in 0.02 M phosphate buffer containing 0.05 NaCl. Urea was obtained from Sigma Chemical Co. and was used without further purification. Urea concentration was determined from refractive index measurements (Pace, 1986).

Methods

Circular dichroism spectra were recorded at room temperature with an AVIV 62DS instrument (Aviv Associates, Lakewood, NJ) using a 0.02 cm path length. The protein concentration was in the range 30−50 μM. No aggregation was found to occur within this range, either in the native or in the unfolded state (Carra et al., 1994a). The spectra shown represent the average of three experimental curves.

The unfolding transitions were monitored using an AVIV 62DS spectropolarimeter to which a second photomultiplier has been adapted at right angle for fluorescence measurements. In this arrangement, CD and fluorescence data for the same sample can be obtained almost simultaneously. The instrument and the data acquisition protocol were described in detail elsewhere (Ramsay & Eftink, 1994; Ramsay et al., 1995). All the experiments were done at 20 °C, the temperature being controlled by a thermoelectric cell holder. The pH measurements were performed with an ORION pH meter (model 720A) having a combination pH electrode. The cells used were 1 cm × 1 cm, and the protein concentration was in the range 3−5 μM. The fluorescence unfolding profile was obtained with an excitation wavelength of 295 nm, and the emission at 340 nm was selected by an interference filter.

For urea-induced unfolding experiments, the spectrophotometer was coupled to a computer-controlled syringe pump, so that an unfolding profile was automatically recorded. The accuracy of the titration was checked at the end of each experiment; the difference between the measured and the calculated final urea concentration never exceeded 0.1 M. In order to assure that equilibrium was reached after each denaturant injection, a subroutine for signal equilibration was run prior to data acquisition (Ramsay et al., 1995). Early experiments revealed that addition of urea increases the measured pH of aqueous solutions (Bull et al., 1964). For phosphate buffer, we found a linear dependence of pH on urea concentration in the range 0−2 M, when the starting pH was around 4.5, 5.5, and 6.5, with a larger variation (4%) for the lower pH range. This dependence was extrapolated to higher urea concentrations, at which the pH electrode becomes unresponsive (Yao & Bolen, 1995).

For the acid-induced unfolding experiments, a computer-controlled pH meter was included in the system. The syringe was filled with 1 N HCl, and the pH was automatically adjusted as described in Ramsay et al. (1995), in order to collect data at evenly spaced pH intervals. The volume of each acid aliquot was recorded to calculate protein and urea concentration at every pH. The dilution at the end of each experiment was less than 10%.

At a particular set of experimental conditions (pH and urea concentration), the signal (either CD or fluorescence) was measured for 25 s, with an integration time of 1 s. The average and standard deviation of the 25-values set were calculated, corrected for protein concentration, and stored together with the urea and pH values for further global analysis.

For each protein studied (WT, V66W′, or V66W), 12 unfolding profiles were globally analyzed. These correspond to three acid-induced unfoldings (at different urea concentrations) and three urea-induced unfoldings (at different pH values) for two different signals (CD and fluorescence). The number of experimental points was 390 for WT, 437 for V66W, and 310 for V66W′. We used a two-state model for WT and V66W′ and a three-state model for V66W; these models will be described below.

Thermodynamic Model. A two-state model implies that the unfolding occurs only between two states, native (N) and unfolded (U), with any other intermediate forms being less stable than either N or U, so that their population can be considered negligible. For the reaction N $\rightleftarrows$ U, the equilibrium constant is K_{UN} = [U]/[N], and the free energy change for unfolding is $\Delta G^\circ_{UN} = -RT \ln K_{UN}$.

A thermodynamic model should describe the dependence of the free energy change, ΔG°_{UN}, on the denaturant concentration. According to Tanford (Aune & Tanford, 1969), the effects of urea and pH can be considered, to a first approximation, to be independent, so that

$$\Delta G^\circ_{UN} = \Delta G^\circ_{0,UN} - f(\text{pH}) - g([\text{urea}]) \qquad (1)$$

In this equation, $\Delta G^\circ_{0,UN}$ is the difference in standard free energy between the unfolded and the folded states in the absence of urea and at a pH where both states are fully unprotonated, and f and g are two different functions that depend on pH and urea concentration, respectively.

A general expression for f(pH) has been given by Tanford (1970), considering that the pH dependence of the free energy is determined solely by the titratable groups that have different pK_a's in the native and unfolded states. If the groups titrate independently, f(pH) has the expression:

$$f(\text{pH}) = RT\sum_{i=1}^{n} \ln \frac{1 + 10^{-\text{pH}+\text{p}K_{a,U_i}}}{1 + 10^{-\text{pH}+\text{p}K_{a,N_i}}} \qquad (2)$$

where pK_{a,U_i} and pK_{a,N_i} are the pK_a of the titratable group "i" in the unfolded and native state, respectively, and n is the number of such titratable groups (having different pK_a values in the native and unfolded states). Barrick and Baldwin (1993) simplified eq 2 to

$$f(\mathrm{pH}) = nRT \ln(1 + 10^{-\mathrm{pH}+\mathrm{p}K_{a,U}}) \quad (3)$$

based on the following assumptions: (1) there is only one type of titratable group; and (2) the titratable groups remain unprotonated in the native state, due to an abnormally low p$K_{a,N}$.

For g([urea]), the function that describes the dependence of the free energy of unfolding on urea concentration, we have used

$$g([\mathrm{urea}]) = m[\mathrm{urea}] \quad (4)$$

as suggested by Pace (1986) and Schellman (1978).

Independent effects of urea and pH imply a constant m value over the entire pH range studied and no dependence of p$K_{a,U}$ on the concentration of urea.

Five cases, corresponding to different dependencies of protein stability on pH and urea, have been considered in the data analysis. Case 1 corresponds to the above model proposed by Barrick and Baldwin, and it was used for all the proteins studied; in cases 2−5, some restrictions imposed by this model are released, in order to determine their effect on the goodness of the fit. Cases 2−5 were considered only in the analysis of the WT data.

Case 1. From eqs 1, 3, and 4, one deduces

$$\Delta G^\circ_{UN} = \Delta G^\circ_{0,UN} - nRT \ln(1 + 10^{-\mathrm{pH}+\mathrm{p}K_{a,U}}) - m[\mathrm{urea}] \quad (5)$$

There are four global thermodynamic parameters ($\Delta G^\circ_{0,UN}$, n, p$K_{a,U}$, and m), and they describe the simplest dependence of ΔG°_{UN} on pH and urea concentration, with m and p$K_{a,U}$ being independent of pH or urea concentration.

Case 2. In this case m was considered to be linearly dependent on urea concentration, $m = m_0 + (\partial m/\partial[\mathrm{urea}]) - [\mathrm{urea}]$, where m_0 is the value of m in the absence of urea and $\partial m/\partial$[urea] represents the dependence of m on denaturant concentration. There are five global parameters ($\Delta G^\circ_{0,UN}$, n, p$K_{a,U}$, m_0, and $\partial m/\partial$[urea]) and

$$\Delta G^\circ_{UN} = \Delta G^\circ_{0,UN} - nRT \ln(1 + 10^{-\mathrm{pH}+\mathrm{p}K_{a,U}}) - \left(m_0 + \frac{\partial m}{\partial[\mathrm{urea}]}[\mathrm{urea}]\right)[\mathrm{urea}] \quad (6)$$

Case 3. This case corresponds to m being linearly dependent on pH, $m = m_0 + (\partial m/\partial\mathrm{pH})\mathrm{pH}$, where m_0 is the value of m at pH 0 and $\partial m/\partial$pH represents the dependence of m on pH. The global parameters are $\Delta G^\circ_{0,UN}$, n, p$K_{a,U}$, m_0, and $\partial m/\partial$pH and

$$\Delta G^\circ_{UN} = \Delta G^\circ_{0,UN} - nRT \ln(1 + 10^{-\mathrm{pH}+\mathrm{p}K_{a,U}}) - \left(m_0 + \frac{\partial m}{\partial \mathrm{pH}}\mathrm{pH}\right)[\mathrm{urea}] \quad (7)$$

Case 4. The protonation of the native state is taken into account in this case. From eqs 1 and 2, one obtains, assuming that the titratable groups are identical, the following expression for the free energy of unfolding:

$$\Delta G^\circ_{UN} = \Delta G^\circ_{0,UN} - nRT \ln \frac{1 + 10^{-\mathrm{pH}+\mathrm{p}K_{a,U}}}{1 + 10^{-\mathrm{pH}+\mathrm{p}K_{a,N}}} - m[\mathrm{urea}] \quad (8a)$$

If one defines $\delta = \mathrm{p}K_{a,U} - \mathrm{p}K_{a,N}$, then eq 8a can be rewritten as

$$\Delta G^\circ_{UN} = \Delta G^\circ_{0,UN} - nRT \ln \frac{1 + 10^{\mathrm{pH}-\mathrm{p}K_{a,U}}}{10^{-\delta} + 10^{\mathrm{pH}-\mathrm{p}K_{a,U}}} - m[\mathrm{urea}] \quad (8b)$$

Thus, the value of δ represents the shift in pK_a of the side chain that occurs upon acid-induced unfolding. In case 4, the global parameters are $\Delta G^\circ_{0,UN}$, n, p$K_{a,U}$, m, and δ.

Case 5. This model is for the situation when the titratable groups are not "identical"; that is, they do not have the same pK_a in the unfolded state. If the acid unfolding is triggered only by aspartates and glutamates, which have a pK_a around 4, the assumption that the titratable groups are identical is not very drastic. The situation is different if some histidine residues (pK_a around 6) are also involved in the unfolding. NMR studies (Alexandrescu et al., 1988) have shown that His^{121} of WT SNase has a relatively low pK_a of 5.5 in the native state. If the titratable groups of SNase can be divided into two subgroups, (a) aspartates and glutamates, which do not become protonated in the native state, and (b) one perturbed histidine, which can be protonated in both the native and the unfolded state, then from eqs 1−4 one obtains

$$\Delta G^\circ_{UN} = \Delta G^\circ_{0,UN} - nRT \ln(1 + 10^{-\mathrm{pH}+\mathrm{p}K_{a,U}}) - RT \ln \frac{1 + 10^{-\mathrm{pH}+\mathrm{p}K_{a,U}^{His}}}{1 + 10^{-\mathrm{pH}+\mathrm{p}K_{a,N}^{His}}} - m[\mathrm{urea}] \quad (9)$$

Using for $\mathrm{p}K_{a,N}^{His}$ a fixed value of 5.5, the global parameters for this case are $\Delta G^\circ_{0,UN}$, n, m, p$K_{a,U}$ (the pK_a of aspartates or glutamates in the unfolded state), and $\mathrm{p}K_{a,U}^{His}$ (the pK_a of the histidine in the unfolded state).

The three-state model, N ⇄ I ⇄ U, considers that an equilibrium intermediate becomes significantly populated. There are two equilibrium constants involved, $K_{IN} = [\mathrm{I}]/[\mathrm{N}]$ and $K_{UI} = [\mathrm{U}]/[\mathrm{I}]$. If the p$K_a$'s of the titratable groups involved in the first transition are the same in the intermediate and unfolded states ($\mathrm{p}K_{a,I1} = \mathrm{p}K_{a,U1}$), then the dependencies of the free energy differences on pH and urea are given by (Barrick & Baldwin, 1993)

$$\Delta G^\circ_{IN} = \Delta G^\circ_{0,IN} - n_1 RT \ln(1 + 10^{-\mathrm{pH}+\mathrm{p}K_{a,I1}}) - m_1[\mathrm{urea}] \quad (10)$$

$$\Delta G^\circ_{UI} = \Delta G^\circ_{0,UI} - n_2 RT \ln(1 + 10^{-\mathrm{pH}+\mathrm{p}K_{a,U2}}) - m_2[\mathrm{urea}] \quad (11)$$

where n_1 and n_2 represent the number of titratable groups involved in the N ⇄ I and I ⇄ U transitions, respectively, p$K_{a,I1}$ is the pK_a in the I state of the groups responsible for the first transition ($\mathrm{p}K_{a,I1} = \mathrm{p}K_{a,U1} \gg \mathrm{p}K_{a,N1}$), and p$K_{a,U2}$ is the pK_a in the U state of the groups that are responsible for the second transition ($\mathrm{p}K_{a,U2} > \mathrm{p}K_{a,I2}$, $\mathrm{p}K_{a,N2}$).

Data Fitting. If the N and U states have different signals, Y_N and Y_U, respectively, then the measured signal Y is an average over the two populations, $Y = X_N Y_N + X_U Y_U$; X_N and X_U represent the mole fraction of each state, and for a two-state transition, they are given by the following relationships:

$$X_N = \frac{1}{1 + K_{UN}}; \quad X_U = \frac{K_{UN}}{1 + K_{UN}} = 1 - X_N \qquad (12)$$

As a denaturing agent is added, the difference in free energy between the two states changes. This will affect the fractional occupation of each state, so that, for example, an unfolding profile starts with a signal characteristic for the native state ($X_N \approx 1$) and ends with a signal characteristic of the unfolded state ($X_U \approx 1$). Our fitting program takes also into account a linear dependence of the intrinsic signals Y_N or Y_U on the denaturing agents through the relationships:

$$Y_N = Y_N^0(1 + \alpha_N^Y \mathrm{pH} + \beta_N^Y[\mathrm{urea}])\gamma_i \qquad (13a)$$

$$Y_U = Y_U^0(1 + \alpha_U^Y \mathrm{pH} + \beta_U^Y[\mathrm{urea}])\gamma_i \qquad (13b)$$

where Y^0 is the value of the signal at pH 0 and [urea] = 0, α^Y and β^Y are the relative slopes that describe the dependence of the signal Y on pH and [urea], respectively, and γ_i is a scaling factor. When several data sets are simultaneously fitted, we considered it more suitable to use "relative" values for the slopes α^Y and β^Y in order to minimize, as much as possible, the dependence of these parameters on the absolute value of the signal Y. In our global analysis of 12 unfolding profiles, Y is the CD signal at 222 nm for 3 profiles, the CD signal at 228 nm (at 235 nm for V66W′) for 3 profiles, and the fluorescence intensity for 6 profiles. Thus, the slopes and intercept represent linking parameters among a group of three, or another group of three, or a group of six, respectively, experimental curves. Due to the inherent experimental errors in determining the molar value of the signal Y (e.g., due to irreproducibility in alignment, determination of the protein concentration, lamp intensity, etc.), the above linkage requires some "scaling" factors γ for the amplitudes. For a group of three curves, one needs two scaling factors, and for a group of six curves, one needs five scaling factors.

In summary, for wild type, the 12 unfolding profiles were fitted with 31 (or 32, depending on the thermodynamic model) fitting parameters, including 4 (or 5) global thermodynamic parameters, 6 Y^0 values, 6 α^Y values, 6 β^Y values, and 9 scaling factors. None of these fitting parameters can be considered "local" for an individual data set. For V66W′, the slope of the CD signal at 235 nm of the unfolded state and the slope of the CD signal at 222 nm of the native state were poorly defined, so we reduced the number of fitting parameters to 27, by setting $\alpha_U^{CD235} = \beta_U^{CD235} = 0$ and $\alpha_N^{CD222} = \beta_N^{CD222} = 0$. The thermodynamic parameters obtained with these slopes differ by less then 2% from the thermodynamic parameters recovered with the above slopes fixed at the values of those of the wild type.

For a three-state model N ⇄ I ⇄ U, the partition function is $Q = 1 + K_{IN} + K_{IN}K_{UI}$, and the mole fraction of each species is

$$X_N = 1/Q \qquad (14a)$$

$$X_I = K_{IN}/Q \qquad (14b)$$

$$X_U = 1 - X_N - X_I \qquad (14c)$$

The measured signal in this case is $Y = X_N Y_N + X_I Y_I + X_U Y_U$, where Y_I is the characteristic signal for the intermediate species. Y_N and Y_U are described by the same relationships as in the two-state model, and Y_I is

$$Y_I = Y_I^0(1 + \alpha_I^Y \mathrm{pH} + \beta_I^Y[\mathrm{urea}])\gamma_i \qquad (15)$$

We further assumed that the slopes of the intermediate state signal are averages of the slopes for the native and unfolded state signals:

$$\alpha_I^Y = \frac{\alpha_N^Y + \alpha_U^Y}{2}; \beta_I^Y = \frac{\beta_N^Y + \beta_U^Y}{2} \qquad (16)$$

The number of fitting parameters increases for a three-state model compared to a two-state model by 7; these include four additional thermodynamic global parameters and three Y_I's (the signal of the intermediate state at pH 0 and [urea] = 0 for CD at 228 nm, CD at 222 nm, or fluorescence, respectively).

The fittings were performed with the NONLIN program (Johnson & Fraiser, 1985), and confidence intervals were evaluated at 67%. In all the analyses, the variance of the fit, χ^2, was used as an indicator of the goodness of the fit (ideally, $\chi^2 = 1$). In order to calculate χ^2, the fitting program requires the standard deviation of each experimental point. The standard deviation for each measured point has been evaluated experimentally as described under Methods.

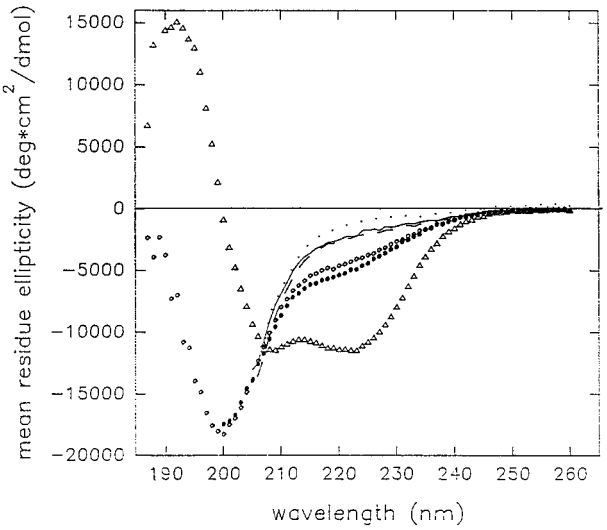

FIGURE 1: CD spectra of wild-type SNase in 0.02 M phosphate buffer, 0.05 M NaCl, 20 °C; (△) pH 7.4; (○) pH 2.0; (●) pH 0.5; (—) pH ≈1.5 and 6 M urea; (- - -) pH ≈7 and 6 M urea; (···) pH ≈2 and 6 M GuHCl.

RESULTS

Wild-Type SNase. Figure 1 presents the CD spectra for WT in native and denaturing conditions. As can be seen, decreasing the pH below 2 changes the acid-induced unfolded state, due to the formation of the A-state (Carra et al., 1994b). The A-state of SNase has a relatively compact size, substantial non-native secondary structure, and little or no tertiary structure (Fink et al., 1993). Since the analysis of the unfolding profiles is limited to the pH range 2−7.5 and the experiments were done at low ionic strength, the contribution of the A-state is not taken into account in the data analysis. The CD spectra of the acid-induced and urea-induced unfolded states are different, suggesting that more residual structure is present in the first case. No differences

Table 1: WT SNase Secondary Structure Content

state	data type	program	α (%)	β (%)	other (%)	reference
native	CD	SELCON[a]	35	30	35	this paper
	CD	K2D[b]	26	15	59	this paper
	CD	LINCOMB[c]	36	16	48	this paper
	CD	CHANG[d]	22	38	40	Chen et al. (1991)
	X-ray		27	39	34	Fink et al. (1993)
	FTIR		25	44	32	Fink et al. (1993)
acid-unfolded	CD	SELCON	5	38	57	this paper
state[e]	CD	K2D	7	26	67	this paper
	CD	LINCOMB	16	8	76	this paper
	CD	CHANG	−	52	48	Chen et al. (1991)
urea-unfolded	CD	SELCON	10	48	42	this paper
state[f]	CD	K2D	6	42	52	this paper
	CD	LINCOMB	12	20	68	this paper

[a] Sreerama & Woody (1993). [b] Andrade et al. (1993). [c] Perczel et al. (1992). [d] Chang et al. (1978). [e] pH 2.0. [f] 4M urea.

were found between the spectra recorded in the presence of high urea concentration at high and low pH. It is interesting to note the differences between the spectra of the urea- and GuHCl-induced unfolded forms.

The deconvolution of the CD spectra using different programs provides results for the native state that are in agreement with previous reported data (Chen et al., 1991; Fink et al., 1993). Analysis of the unfolded state provides questionable results, probably due to the contribution of the aromatic residues, to the poor definition of a β-sheet spectrum in the basis spectra, and to the narrow wavelength range (205−260 nm) accessible for investigation in the presence of urea. The persistence of a compact structure in the unfolded state cannot be excluded (Shortle & Meeker, 1986; James et al., 1992). Results of the CD deconvolution are shown in Table 1.

The unfolding profiles for WT using acid or urea as denaturants are shown in Figure 2. For the acid-induced unfolding (Figure 2A), the midpoint of transition shifts to higher pH values, and the cooperativity of transition decreases slightly as the unfolding occurs in the presence of higher urea concentrations. For urea-induced unfolding (Figure 2B), the midpoint of transition shifts to lower urea concentration when the unfolding occurs at lower pH.

Independent of the denaturant used, the profile shapes are characteristic of a two-state transition. The results of the global analysis over 12 curves are shown in Table 2. The thermodynamic model used was described under Materials and Methods. In case 1, the four global fitting parameters were the same as those considered for a two-state transition by Barrick and Baldwin (1993). The free energy of unfolding $\Delta G^\circ_{0,UN} = 6.2$ kcal/mol and the m value of 2.6 kcal mol^{-1} M^{-1} are in good agreement with previously reported values (Sugawara et al., 1991; Creighton & Shortle, 1994). There seems to be three or four groups that trigger the pH unfolding, and these groups have a pK_a close to that expected for aspartic or glutamic acid. A relatively good fit was obtained for the acid-induced unfolding curves, but the urea unfolding profiles show larger deviations between the calculated and experimental points ($\chi^2 = 42.79$, see the dashed lines in Figure 2).

Several constraints of the model were released, in order to see which would significantly improve the goodness of the fit (see Table 2). In case 2, m was considered to be linearly dependent on urea concentration, as Johnson and Fersht (1995) found for barnase. The χ^2 decreased, but not very much. The χ^2 decreased considerably ($\chi^2 = 13.18$) in case 3, when m was considered to be linearly dependent on pH. A linear dependence of m on pH was chosen as the simplest possible pH dependence of a thermodynamic parameter, and this is experimentally supported by results obtained on ribonuclease A (Pace et al., 1990). In case 4, it is considered that the titratable groups can exist in both protonated and unprotonated forms in the native state of the protein. The parameter δ, which was described under Materials and Methods, represents the difference between the pK_a of the titratable groups in the unfolded and native state of the protein. If δ is allowed to float and p$K_{a,U}$ is fixed at the value 4.6 (an expected value for a glutamic acid side chain in an unfolded protein) the result of the fit is $\delta = 1.06$ (see Table 2). The χ^2 for this fit is larger than the values obtained for the other cases, and the χ^2 increases if the fixed value for p$K_{a,U}$ is lowered.

Case 5, in which the contribution of one histidine residue is taken into account, resulted in a global fit that is even better than that obtained for case 3; the χ^2 for the fit in case 5 is 12.33. In this fit, the pK_a of the considered histidine residue increases from 5.5 [a fixed value, to correspond to the value from the NMR data of Alexandrescu et al. (1988)] to 6.7 upon unfolding, and the p$K_{a,U}$ for the other perturbed groups was found to be 4.4, a value that is characteristic for glutamates or aspartates. The fit in case 5 results in a small increase in $\Delta G^o_{0,UN}$ compared to the values obtained when all the groups were considered identical. The increase in $\Delta G^\circ_{0,UN}$ to 6.6 kcal/mol reflects the fact that the free energy change, according to this model, is defined for the transition between the fully unprotonated U and N states; from eq 9 and the values in Table 2, one obtains $\Delta G^\circ_{UN} = 6.4$ kcal/mol at pH 7.

V66W′. In Figure 3 are shown the unfolding curves for V66W′. For the acid-induced unfolding (Figure 3A), the CD signal at 235 nm decreases in absolute value upon unfolding. This direction of change in CD signal may be somewhat surprising, but, according to the characteristic spectra of α-helix, β-sheet, and random coil, reported by Chang and co-workers (1978), the CD signal at 235 nm can become more negative as a predominant β-sheet structure is converted to a random coil. The fluorescence shows an increase in the range pH 7−4, followed by a marked decrease between pH 4 and 2. The variation of fluorescence intensity around pH 5 is not sensitive to addition of urea (the midpoint does not shift in the presence of denaturant), so we attribute it to minor changes in the environment of Trp^{66} caused by protonation of a neighboring group. The CD signal changes occur only in the region where the fluorescence intensity decreases. The global analysis for this protein was performed only in the pH range 2−4.5, assuming that only one native-like state is populated at pH 4.5. The urea-induced unfolding of V66W′ (Figure 3B) shows, for the pH domain 4.5−6.5, almost no dependence of the transition midpoint on pH. The thermodynamic parameters obtained from a global fitting of the experimental curves shown in Figure 3 are presented in Table 2. The fit for V66W′ was very good ($\chi^2 = 5.01$), so we did not consider other versions of the basic model to improve the fit. For this fragment, the analysis yields $\Delta G^o_{0,UN} = 1.6$ kcal/mol and $m = 1.2$ kcal mol^{-1} M^{-1}; the number of titratable groups, compared to that in WT, is decreased by one, and the p$K_{a,U}$ value is smaller for V66W′.

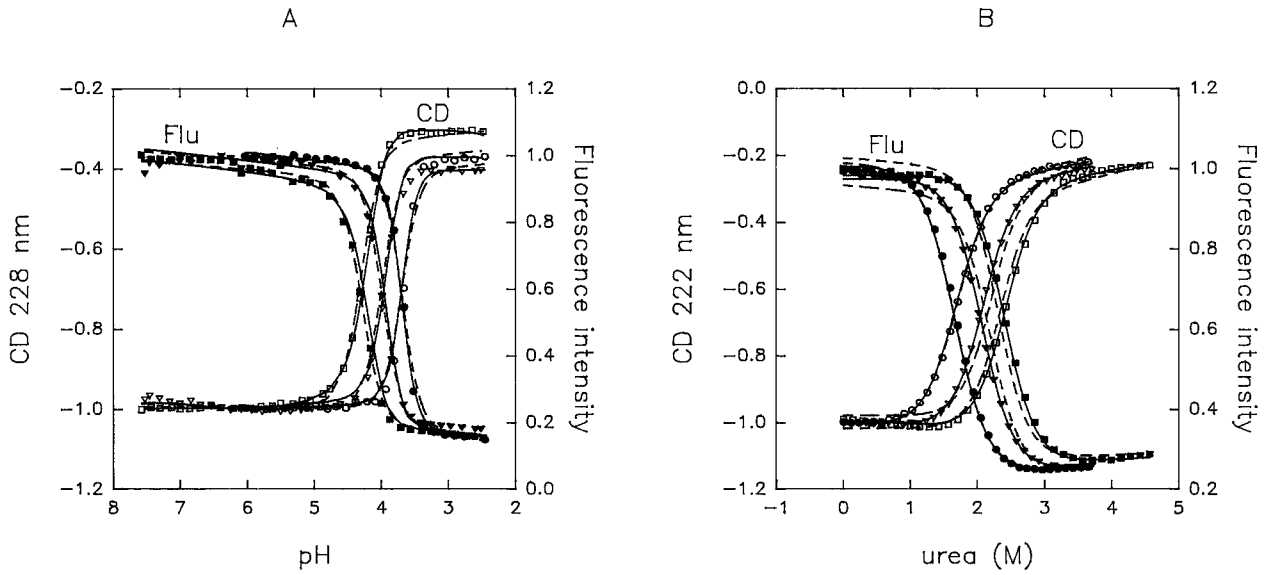

FIGURE 2: (A) Acid-induced unfolding of wild-type SNase at different initial urea concentrations of 0 M (circles), 0.50 M (triangles), and 1.0 M (squares). (B) Urea-induced unfolding of wild-type SNase at different initial pHs of 4.7 (circles), 5.5 (triangles), and 6.5 (squares). In both panels A and B, open symbols represent CD data, and filled symbols represent fluorescence data. In order to reflect better the relative change of the signal upon unfolding, the CD amplitudes were normalized so that the amplitude of the native state corresponds to a value of −1. For absolute values, refer to Figure 1. The experiments were done in 0.02 M phosphate buffer, 0.05 M NaCl, at 20 °C. The dashed lines are curves obtained using the fitting parameters listed in Table 2, case 1, and the solid lines are curves obtained using the fitting parameters listed in Table 2, case 5.

Table 2: Thermodynamic Parameters of Unfolding of Wild-Type SNase and V66W', As Resulted from Global Analysis[a]

protein	case	$\Delta G°_{0,UN}$ (kcal/mol)	n	p$K_{a,U}$	m (kcal mol^{-1} M^{-1})	additional parameter	χ^2
wild type	1	6.26	3.42	5.02	2.66		42.79
		(6.01−6.50)	(3.29−3.56)	(4.95−5.10)	(2.56−2.77)		
	2	6.47	3.70	4.95	2.99[a]	$\partial m/\partial$[urea] = −0.10 kcal mol^{-1} M^{-1}	42.22
		(6.11−6.84)	(3.52−3.88)	(4.88−5.02)	(2.84−3.13)		
	3	5.17	5.13	4.33	3.98[c]	$\partial m/\partial$pH = −0.27 kcal mol^{-1} M^{-1}	13.18
		(4.97−5.36)	(4.82−5.43)	(4.27−4.41)	(3.89−4.07)		
	4	6.16	6.40	4.60	2.70	δ[d] = 1.06	64.81
		(5.87−6.45)	(5.78−7.01)	(fixed)	(2.55−2.86)		
	5	6.63	4.58	4.42	2.55	p$K_{a,U}^{His}$ = 6.74	12.33
		(6.45−6.81)	(4.34−4.84)	(4.34−4.49)	(2.50−2.60)		
V66W′		1.59	2.63	3.38	1.19		5.01
		(1.39−1.79)	(2.29−2.98)	(3.28−3.49)	(1.14−1.23)		

[a] The values in parentheses are the 67% confidence intervals. [b] At 0 M urea. [c] At pH = 0. [d] δ = p$K_{a,U}$ − p$K_{a,N}$.

V66W. In Figure 4 are presented CD spectra of the V66W mutant obtained under different conditions. Under native conditions, the spectrum resembles that of the WT, but it has a slightly smaller amount of α-helix. As seen with the WT, there is a tendency for V66W to form an A-state at very low pH (∼0.5); the CD spectrum of the latter form is completely different from that found at pH 3.7. In Figure 4 is also shown the CD spectrum of the fragment V66W′ at pH 3.4, which almost superimposes on the spectrum obtained for the full-length V66W mutant at a similar pH.

The acid- and urea-induced unfolding curves for V66W are shown in Figure 5. The presence of an equilibrium intermediate is clearly seen in the pH-induced unfolding profiles (Figure 5A) by both CD and fluorescence signals. In the urea-induced unfolding (Figure 5B), there are also deviations from a two-state profile. The poor fit of the two-state model (case 1) is evidenced by the large $\chi^2 = 81$ in Table 3. The deviations from two-state are clearly seen as a nonrandom plot of the residuals, the differences between the experimental and calculated values, for each of the data sets [residual plots not shown; but see Eftink et al. (1996) for an example]. The presence of an equilibrium intermediate during GuHCl unfolding was first reported by Gittis et al. (1993). Later, from calorimetric studies, Carra et al. (1994c) found that the thermal unfolding of V66W comprises two successive first-order phase transitions. Neither the differential scanning microcalorimetry profile nor the denaturant-induced unfolding profile shows a well-defined peak for the intermediate as is seen in the acid-induced unfolding.

A global fit was then performed for this protein using a three-state model, as described under Materials and Methods. The fitting parameters are given in Table 3. In case a, the parameters describing the second transition (I ⇄ U) were fixed at values obtained for the unfolding of V66W′. This constraint assumes that the second transition for V66W is due to the unfolding of the β-barrel subdomain, which is equivalent to the main structural component of V66W′. The fitting curves shown in Figure 5 and the variance of the fit of 17.35 support this equivalence hypothesis. Even though this is not direct proof that the intermediate formed during the unfolding of V66W is thermodynamically similar to the native state of V66W′, the global analysis strongly suggests this to be so.

In case b, all the parameters were allowed to float. One can see that the changes of the fitting parameters from case a to case b are small. Moreover, χ^2 drops from 17.35 in the

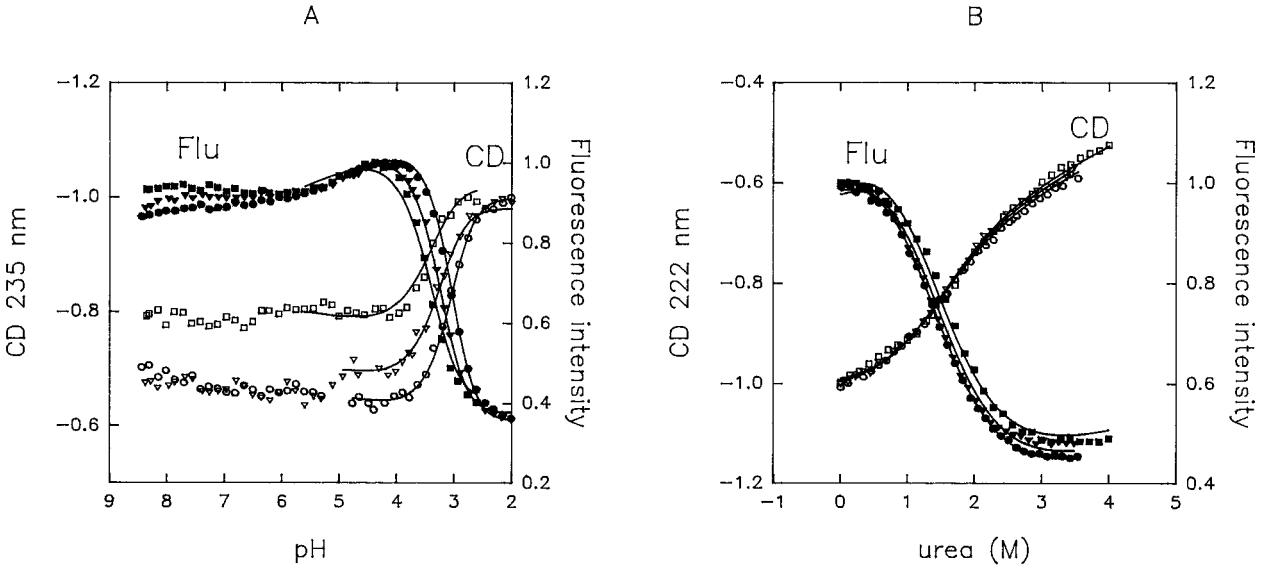

FIGURE 3: (A) Acid-induced unfolding of SNase fragment V66W′ at different initial urea concentrations of 0 M (circles), 0.46 M (triangles), and 0.87 M (squares). (B) Urea-induced unfolding of SNase fragment V66W′ at different initial pHs of 4.7 (circles), 5.5 (triangles), and 6.5 (squares). In both panels A and B, open symbols represent CD data, and filled symbols fluorescence data. The CD amplitudes were normalized so that the amplitude of the unfolded state corresponds to a value of −1 in panel A, and the amplitude of the native state corresponds to a value of −1 in panel B. The experiments were done in 0.02 M phosphate buffer, 0.05 M NaCl, at 20 °C. The lines are the curves resulting from the global analysis using the parameters listed in Table 2.

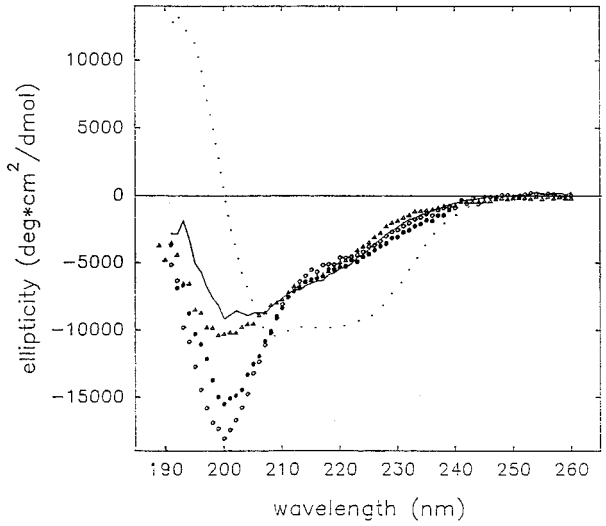

FIGURE 4: CD spectra of V66W mutant of SNase in 0.02 M phosphate buffer, 0.05 M NaCl at 20 °C; (···) pH 7.4; (—) pH 3.7; (○) pH 1.8; (●) pH 0.5; (△) CD spectrum of SNase fragment V66W′ at pH 3.4. The CD spectrum of V66W′ at pH 1.8 is the same as that of V66W at pH 1.8.

first case to 16.42 for the second case, which is not significant, considering that four additional parameters were introduced. As listed in Table 3, the N ⇄ I and the I ⇄ U transitions have similar values of *m*, with $\Delta G°_{0,IN}$ being slightly larger than $\Delta G°_{0,UI}$. The number of titratable groups is not equally distributed for the N ⇄ I and I ⇄ N transitions for V66W. There is one titratable group associated with the first transition (with a high pK_a value) and two or three with the second (pK_a value close to that for aspartic or glutamic acid).

Using the thermodynamic parameters obtained in case a for V66W and eq 14b, we have calculated the mole fraction of the intermediate species at different pH and urea values. The results are shown in Figure 6. The same surface is rotated to show two perspectives. One can see that the maximum population of the intermediate state during urea-induced unfolding is about 20% (at pH 7.0, 1.6 M urea) and that the maximum population reached during the acid-induced unfolding is about 75% (at pH 3.8, 0.2 M urea). The high population of the intermediate state, together with a favorable spread of the signals corresponding to the native, intermediate, and unfolded states, may explain why the three-state unfolding process is easier to observe in the acid-induced unfolding.

DISCUSSION

In this study, we attempted to use a single thermodynamic model to describe the effect of two denaturing agents (acid and urea) on the stability of a protein. The global analysis that we performed on each of the proteins involves a simultaneous fit of six CD profiles (as an indicator of the secondary structure content) and six fluorescence profiles (as an indicator of the local environment of tryptophan residues). There are two major advantages of the global analysis, as compared to analysis of individual data sets. First, the fitting parameters can be recovered with smaller uncertainties, and second, different physical models can be more easily distinguished according to their capability to describe the entire set of data (Beechem et al., 1991).

Early studies on protein folding (Epstein et al., 1971a) found that the acid-induced unfolding of WT SNase is reversible. More recent studies (Sugawara et al., 1991; Carra et al., 1994a) have confirmed that both the acid-induced unfolding (at low ionic strength) and the urea-induced unfolding are reversible processes for WT SNase, and that, in both cases, no significantly populated intermediates are formed.

We have used what Barrick and Baldwin (1993) have called "the simplest model, containing the minimal number of parameters" to simultaneously describe the urea- and acid-induced CD and fluorescence unfolding profiles. Nevertheless, this model is based on certain assumptions. The first assumption is that the acid-induced and urea-induced unfolded states are thermodynamically equivalent; that is, they

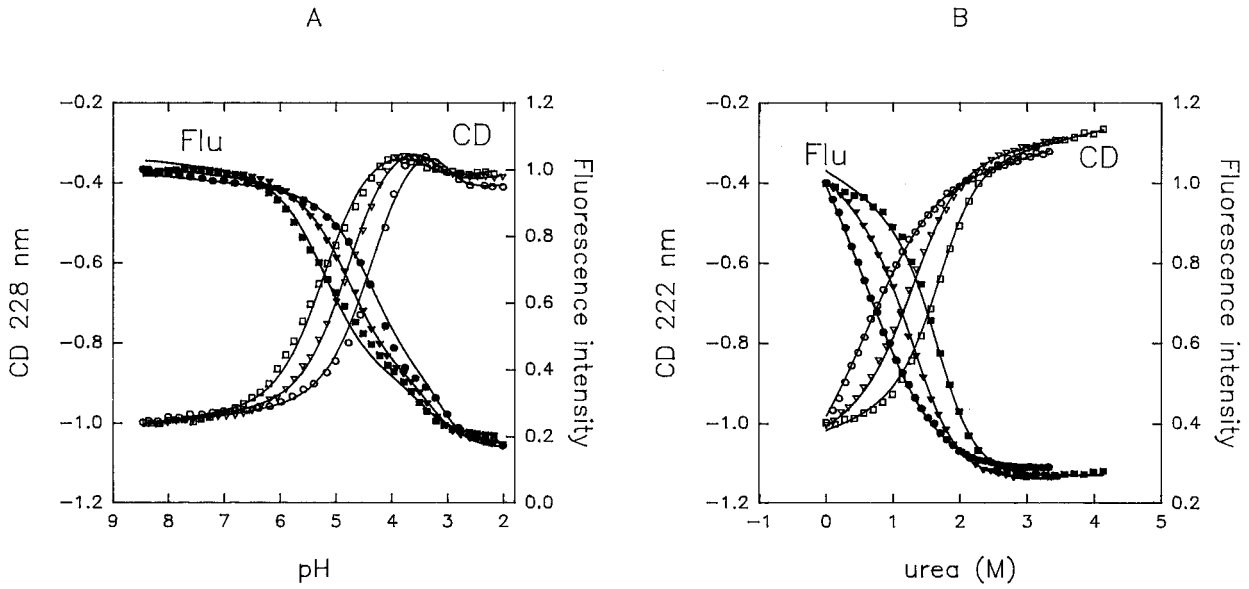

FIGURE 5: (A) Acid-induced unfolding of V66W SNase mutant at different initial urea concentrations of 0 M (circles), 0.50 M (triangles), and 0.97 M (squares). (B) Urea-induced unfolding of V66W SNase mutant at different initial pHs of 4.7 (circles), 5.5 (triangles), and 6.5 (squares). In both panels A and B, open symbols represent CD data, and filled symbols fluorescence data. The CD amplitudes were normalized so that the amplitude of the native state corresponds to a value of −1. The experiments were done in 0.02 M phosphate buffer, 0.05 M NaCl, at 20 °C. The lines are the curves which result from the global analysis using the parameters listed in Table 3, case a.

Table 3: Thermodynamic Parameters of Unfolding for V66W, As Resulted from the Global Analysis[a]

two-state fit	$\Delta G°_{o,UN}$ (kcal/mol)	n	pK_a	m (kcal mol^{-1} M^{-1})					χ^2
case 1	1.96 (1.79−2.15)	0.79 (0.70−0.87)	6.01 (5.88−6.14)	1.18 (1.06−1.30)	(1.06−1.30)	(1.06−1.30)	(1.06−1.30)	(1.06−1.30)	81.3 (1.06−1.30)
three-state fit	$\Delta G°_{o,IN}$ (kcal/mol)	n_1	p$K_{a1,I}$	m_{IN} (kcal mol^{-1} M^{-1})	$\Delta G°_{o,UI}$ (kcal/mol)	n_2	p$K_{a2,U}$	m_{UI} (kcal mol^{-1} M^{-1})	χ^2
case a	2.70 (2.49−2.90)	1.04 (0.96−1.12)	6.25 (6.15−6.36)	1.14 (1.07−1.21)	1.60 (fixed)	2.64 (fixed)	3.39 (fixed)	1.19 (fixed)	17.35 (fixed)
case b	2.78 (2.54−3.04)	1.06 (0.99−1.14)	6.29 (6.18−6.41)	1.25 (1.16−1.33)	2.21 (1.80−2.61)	2.37 (1.85−2.93)	3.66 (3.45−3.87)	1.40 (1.22−1.58)	16.42 (1.22−1.58)

[a] The values in parentheses are the 67% confidence intervals.

have the same free energy under ***native*** conditions. In other words, the model embodied by eq 1 assumes that $\Delta G°_{0,UN}$ is the same when extrapolated back to native conditions along either the pH or the [urea] axis (or a combination thereof). If the acid- and urea-induced unfolded forms are different thermodynamic states, this should be a three-state model. The Occam's razor approach is to assume a single unfolded thermodynamic state, unless the data show a convincing deviation from the two-state model. Further, our strategy of monitoring the unfolding transition by a combination of CD and fluorescence signals is designed to try to detect deviations from a two-state model. On a related matter, the small spectral differences observed in Figure 1 between the low pH and high urea forms of the protein need not indicate the existence of two thermodynamically distinct unfolded states for the following reasons: (i) the CD spectra recorded at any points along two perturbation axes (e.g., at any particular low pH or high [urea]) correspond to different values of $\Delta G°_{UN}$ (i.e., different degrees of destabilization with respect to the native state); and (ii) adding urea to an acid-unfolded protein sample induces a gradual change in the CD signal (data not shown), not a sigmoidal shape as would be expected for a transition between two thermodynamically distinct states. We consider this shift in the CD signal to have two possible causes: a redistribution of the populations within the ensemble of the unfolded state configurations and an intrinsic dependence of the CD signal of the unfolded protein on urea concentration.

Another assumption of the simplest model (case 1) is that the effects of acid and urea are independent. In the other versions of the two-state model (cases *2*−5), some of the constraints imposed by this assumption were released. As will be discussed below, this led to a significant improvement of the goodness of fit.

Finally, there is a set of assumptions made in order to express the explicit dependence of $\Delta G°_{UN}$ on the denaturing agents. A general relationship for the pH dependence of the free energy change for the unfolding of a protein was given by Tanford (1970). We used a simplified form of this relationship, as proposed by Barrick and Baldwin (1993), which assumes that the acid-induced unfolding is caused by the protonation of n identical and independent groups, which have an abnormally low pK_a in the native state. There are different models that can describe the effect of urea on $\Delta G°_{UN}$ (Pace, 1986). We have chosen among these the one that assumes a linear dependence of $\Delta G°_{UN}$ on denaturant concentration, which seems to be followed by urea more so than by guanidine-hydrochloride (Staniforth et al., 1993; Makhatadze & Privalov, 1992). Bolen and Santoro (1988) and Yao and Bolen (1995) have shown that the free energy

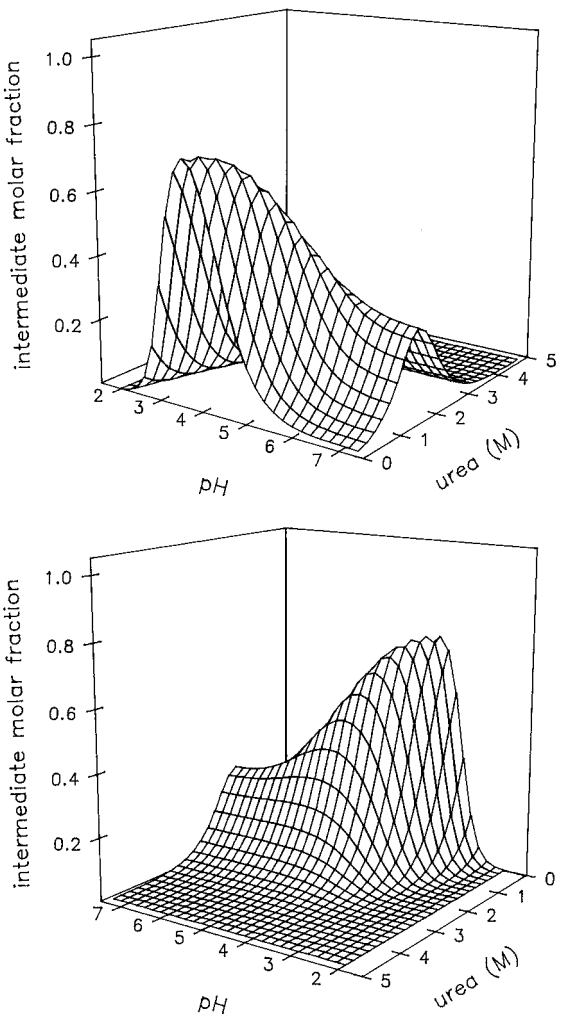

FIGURE 6: Mole fraction of the intermediate of V66W as a function of [urea] and pH. The fraction was evaluated using eq 14b and the fitting parameters shown in Table 3, case a. Two perspectives are shown for the surface. One view (upper graph) is from pH and urea ranges favorable to the native state, and the other view (lower graph) is from pH and urea ranges favorable to the unfolded state.

change in the absence of denaturant, $\Delta G°_{0,UN}$, obtained from the linear-dependence model, has the properties required for a function of state. Their results were obtained from studies on two proteins, α-chymotrypsin (a modified form) and ribonuclease A. We assume that their conclusions extend to SNase.

For WT SNase, the values that we have obtained for $\Delta G°_{0,UN}$ range from 5.2 to 6.6 kcal/mol, depending on the assumptions of the model used to fit the data. These values for $\Delta G°_{0,UN}$ are similar to the values found in the literature (6.3 kcal/mol at 10 °C, pH 8, Creighton & Shortle, 1994; 6.1 kcal/mol at 20 °C, pH 7, Shortle & Meeker, 1986). A more complete list of literature values of $\Delta G°_{0,UN}$ for WT SNase is given in Eftink et al. (1996).

We have found m ($=\partial\Delta G°_{UN}/\partial$[urea]) to be about 2.6 kcal mol^{-1} M^{-1} for the different cases we have studied. Creighton and Shortle (1994) reported a value of $m = 2.5$ kcal mol^{-1} M^{-1} (at 10 °C, pH 8), and Sugawara et al. (1991) reported a value of $m = 2.2$ kcal mol^{-1} M^{-1} (at 4.5 °C, pH 7) for WT SNase. The value 2.6 kcal mol^{-1} M^{-1} is obtained with a model that assumes m to be independent of pH. A larger value is obtained for a fit that assumes m to be linearly dependent on pH. The latter fit gives $m = 3.9$ kcal mol^{-1} M^{-1} at pH 0, and with $\partial m/\partial$pH $= -0.27$ kcal mol^{-1} M^{-1}, one obtains a value of $m = 2.1$ kcal mol^{-1} M^{-1} at pH 7.

Whether or not m depends on pH seems to differ from protein to protein. Previous studies (Pace et al., 1990, 1992) have found a linear (for ribonuclease A) or more complex dependence of m on pH (for ribonuclease T1 and barnase). There is a narrow pH interval accessible for this type of study with SNase. However, the fit improved significantly when m was considered dependent on pH (case 3), although the sharpness of the urea unfolding profiles (which is related to the magnitude of m) does not appear to change significantly over the pH range investigated. SNase is a basic protein with the isoelectric point at 10.3; the net charge varies approximately from +10 at pH 7 to +30 at pH 3.0 (Kálmán et al., 1995). Statistics from over 45 proteins have revealed a strong correlation between m and the amount of protein surface exposed to solvent upon unfolding (Myers et al., 1995). Since we found that m is larger at low pH, this would correspond to a more solvent-accessible conformation of the unfolded state as the net charge of the molecule increases. The same correlation between m and net charge was found by Pace and co-workers (Pace et al., 1990, 1992) for other proteins. In a different approach, Makhatadze and Privalov (1992) concluded that m should decrease with increasing protein stability, which is in accord with our findings that m is smaller at neutral pH than at acidic pH. If the unfolded conformation in 6 M urea becomes more expanded as the pH is lowered, due to a net increase of the protein's charge, this might be expected to be reflected in the CD spectrum. We did not find any difference between the CD spectra in 6 M urea at pH 7 and at pH 1.5 (Figure 1). Similarly, Chen et al. (1991) found no difference between the CD spectra of this protein in 2 M GuHCl at pH 7 and at pH 2.2.

The results of the global analysis suggest that there may be three to five groups that are responsible for the acid-induced unfolding of WT SNase. This number is larger than $n = 1$ that was derived from the pH dependence of the denaturation temperature (Carra et al., 1994a) and also is larger than $n = 2.5$ determined from a previous analysis of a fluorescence unfolding profile (Chen et al., 1991). The assumption that the titratable groups are identical and independent is probably the most questionable aspect of the model described by eq 5. The values that we have obtained for n and p$K_{a,U}$ must represent an average over the groups that trigger the unfolding. The pH dependence of the free energy of unfolding indicates that three to five amino acid side chains do not become protonated in the native state as pH is decreased, so these residues must have an abnormally low pK_a in the native state. The pK_a of acidic residues can be lowered by interaction either with positively charged neighboring groups or with polar, neutral groups. The pK_a shifts are usually within 1 pH unit (Tanford, 1970). However, there are cases in which pK_a shifts larger than 2 pH units have been observed (Oliveberg et al., 1994).

The p$K_{a,U} \approx 4.5$ obtained from the fit indicates that the titratable groups involved are mainly aspartates and glutamates. Out of the four histidine residues of nuclease, only His^{121} has a low pK_a of 5.49 in the native state (Alexandrescu et al., 1988). Our analysis (via case 5) suggests that this residue may be involved in the acid-induced unfolding of SNase. Epstein et al. (1971b) deduced from NMR studies that a local conformational change may occur in the environment of His^{121} during progressive acidification.

Table 4: Acidic Residues That Have the Side Chain Oxygens Participating in Several Hydrogen Bonds[a]

acceptor	atom	donor	atom
Glu[75]	OE1	Lys[9]	NZ[b]
	OE2	His[121]	NE2
	OE2	Tyr[93]	OH
Asp[77]	OD1	Tyr[91]	OH
	OD1	Thr[120]	N
	OD2	Thr[120]	OG1
	OD2	Lys[78]	N
Asp[83]	OD1	Tyr[85]	N
	OD1	Gly[86]	N
	OD1	Arg[87]	N
	OD2	Arg[87]	NE
	OD2	Arg[87]	NH1
Asp[95]	OD1	Lys[70]	N
	OD2	Lys[70]	N
	OD2	Lys[71]	N
Glu[135]	OE1	Gln[131]	NE2
	OE1	Arg[105]	NH1
	OE2	Arg[105]	NH2

[a] Selected from the tables published by Hynes and Fox (1991). [b] Not listed as an H-bond in Hynes and Fox (1991). It was included in the table due to the small distance between OE1 of Glu[75] and NZ of Lys[9].

In order to identify the aspartates and glutamates that may be responsible for the acid unfolding of SNase, we have followed the strategy of Aune and Tanford (1969) and have inspected the structure of nuclease for examples of positive charges in the proximity of carboxyl side-chain groups. Using the program RasMol, we searched the X-ray structure of SNase (Hynes & Fox, 1991) for the nitrogen atoms that are within a sphere of radius 3.5 Å from the side-chain carboxyl oxygens of aspartic or glutamic acids. There are 8 aspartic acids and 12 glutamic acids in the 149 polypeptide chain of WT SNase (since the X-ray structure does not contain the coordinates of residues 142−149, the side chains of Glu[142], Asp[143], and Asp[146] were not included in this analysis). The result of our search provided 14 acidic residues: 10 have *both* carboxyl oxygens at less than 3.5 Å from nitrogen atoms (Asp[19], Asp[21], Asp[77], Asp[83], Asp[95], Glu[52], Glu[67], Glu[75], Glu[129], Glu[135]), and 4 have only 1 carboxyl oxygen in the vicinity of a nitrogen atom (Asp[40], Glu[57], Glu[101], Glu[122]) . Since this approach was not very selective for the particular case of WT SNase, we have added as a supplementary criterion for selection the number of hydrogen bonds in which the carboxyl oxygens participate. Inspecting the list of H-bonds in WT SNase (Hynes & Fox, 1991), we suggest that the following residues may trigger the pH-induced unfolding: Glu[75], Asp[77], Asp[83], Asp[95], and Glu[135]. The list of the H-bonds in which the side-chain oxygens of these residues are involved is given in Table 4. Three of these residues (Asp[77], Asp[83], and Glu[75]) have already been proposed by other authors to have a significant contribution to the protein stability. Wang and Shortle (1995) suggested that protonation of Asp[83] destabilizes the tight turn involving residues 83−87. Carra et al. (1994c) found that an intermediate state becomes significantly populated during thermal unfolding if Glu[75] is mutated to valine and that Asp[77] plays an important role in stabilizing the native state. Shown in Figure 7 is a ball-and-stick representation of Glu[75], Asp[77], Asp[83], Asp[95], and Glu[135], with the carboxyl oxygens shown as spheres. It is interesting to note that four of these residues are clustered within the same region of the protein, along the active-site cleft. His[121] and Arg[105] were also represented to emphasize the coupling between SNase subdomains.

V66W′. Small-angle X-ray scattering studies (Flanagan et al., 1992) have shown that the 1−136 fragment of SNase (without tryptophan substituted at position 66) is compact under physiological conditions, although this fragment was found not to have persistent secondary structure. Alexandrescu and Shortle (1994) performed NMR studies on a similar fragment of SNase, Δ131Δ, as a model of an unfolded protein under nondenaturing conditions. They observed that substitution of Val[66] with a more hydrophobic residue can stabilize the fragment's conformation. Gittis et al. (1993) were the first to report that V66W′ undergoes a cooperative transition upon GuHCl-induced unfolding. Our lab has recently presented (Eftink et al., 1996) a global analysis of data for the GuHCl-induced unfolding of V66W′.

For V66W′, the urea unfolding profiles exhibit a sigmoidal shape, usually associated with a two-state transition. The acid-induced unfolding, monitored by fluorescence, presents a more complex profile. During progressive acidification, there is a slight increase of the fluorescence intensity, and this is not associated with any changes of the CD signal. We did not observe a fluorescence increase during the acid unfolding of WT SNase, but it should be emphasized that the location of the fluorescent reporter group is different in WT (Trp at position 140) compared to V66W′ (Trp at position 66). We assume that the increase of fluorescence for V66W′ is due to minor changes in the Trp[66] environment when a neighboring group becomes protonated. There are two reasons to make this assumption. First, the variation of the fluorescence signal has a titration-like profile; and second, the changes occur in the same pH range in the absence or presence of urea. Since we monitored the unfolding process by the fluorescence intensity at 340 nm, the observed increase may be due to a red shift of the emission spectrum, corresponding to a slight increase in solvent exposure of the indole ring. It is unlikely that the fluorescence increase corresponds to an increase of the quantum yield, because any protonated neighbor would act as a quencher.

The global analysis of CD and fluorescence data (versus pH and urea concentration) for V66W′ provided $\Delta G^{o}_{0,UN} =$ 1.6 kcal/mol and $m = 1.2$ kcal mol^{-1} M^{-1}. The value of the free energy of unfolding that we obtained by simultaneous analysis of CD and fluorescence data is between the values found by individual curve analysis of CD ($\Delta G^{o}_{0,UN} = 1.0$ kcal/mol) and fluorescence ($\Delta G^{o}_{0,UN} = 2.4$ kcal/mol) data by Gittis et al. (1993) for the GuHCl-induced unfolding of this fragment at neutral pH. The number of titratable groups responsible for the acid induced unfolding of V66W′ is two or three (approximately one less than that for the WT), and, based on the value of $pK_{a,U} = 3.4$ obtained from the fit, one may suggest that they are mainly aspartate residues.

V66W. Anfinsen (1972) reported 24 years ago what he called "a striking example of the principle of cooperativity in protein structure". He found that SNase fragments comprising residues 6−48 and 49−149 are structureless in solution, but they associate to form a complex that is extremely similar to that of the native protein. Later, it was proposed by Carra et al. (1994c) that SNase's structure should be considered to be composed of two subdomains, with predominantly α-helix and β-sheet structure, respectively. These subdomains are in contact along the active-site cleft, and the tightness of the structure is maintained by

FIGURE 7: Ribbon drawing of wild-type SNase, according to the X-ray structure resolved by Hynes and Fox (1991). Residues 1−5 and 142−149 are missing. The figure was generated using the program Molscript (Kraulis, 1991). Glu^{75}, Asp^{77}, Asp^{83}, Asp^{95}, and Glu^{122} are shown in ball-and-stick with the side-chain oxygens as spheres. His^{121} and Arg^{105} are shown in ball-and-stick.

electrostatic bonds across the contact region. The bonds may be strongly perturbed at pH ≈4 and high ionic strength or by mutating the residues involved in the salt bridges. If the interaction between the subdomains is weakened, the cooperativity of unfolding of SNase is decreased, and the two-state process N ⇄ U may become a three-state process N ⇄ I ⇄ U, with the intermediate state having the more stable β-barrel subdomain still folded in a native-like manner (Carra et al., 1994c). At pH ≈4 and high salt concentration, WT SNase unfolds in two distinct stages during thermal unfolding (corresponding to the unfolding of the α- and β-subdomains); under the same conditions, a fragment containing residues 1−136 unfolds around the melting temperature at which the β-barrel subdomain unfolds (Griko et al., 1994). The presence of equilibrium intermediates during the unfolding/refolding of a protein has attracted more attention since it was found that such intermediates can resemble the transient species that appear during protein folding (Fink, 1995). Pulsed hydrogen−deuterium exchange studies have revealed that the P117G mutant of SNase (a variant that has proline at position 117 replaced by glycine) has a fast refolding intermediate in which the β-sheet region is modestly protected from exchange, whereas the α-helix regions are not (Jacobs & Fox, 1994). For the same mutant, P117G, the thermal unfolding at low pH and high salt concentration is a three-state process, and structural thermodynamic calculations predict that the most stable equilibrium intermediate is one in which the β-subdomain is almost intact and the rest of the molecule is unfolded (Xie et al., 1994).

Position 66 is at a considerable distance from the interface between the subdomains, and it is very unlikely that the substitution of valine with tryptophan affects the bonds across the contact region. The fact that V66W unfolds in a three-state process may be due to a stabilizing effect of the mutation on the intermediate state (Carra et al., 1994c). V66W possesses two tryptophan residues, each positioned in a different subdomain. From thermal unfolding studies of another SNase mutant, V66L, it was concluded that the first transition (N ⇄ I) is associated with changes of fluorescence originating from Trp^{140} and with large changes of the CD signal, whereas the second transition (I ⇄ U) is monitored only by changes in the fluorescence of Trp^{66} (Carra et al., 1994c, 1995). Our results show that, under certain conditions where the population of intermediate is high (∼75%), both CD and fluorescence reflect the N ⇄ I and I ⇄ U transitions (Figure 5A).

We have performed a three-state analysis of the V66W mutant assuming that the second transition corresponds to the β-barrel unfolding and that the thermodynamic parameters associated with the latter transition are those obtained from the V66W′ study. The fit was good, as can be seen in Figure 5, which strongly supports this hypothesis. The results for V66W show that the free energies of unfolding of the two subdomains are $\Delta G°_{0,IN} = 2.7$ kcal/mol and $\Delta G°_{0,UI} = 1.6$ kcal/mol. These values are very close to those reported by Gittis et al. (1993) for V66W for GuHCl-induced unfolding ($\Delta G°_{0,IN} = 2.3$ kcal/mol, $\Delta G°_{0,UI} = 1.7$ kcal/mol). These authors also found a close agreement between the thermodynamic parameters describing the second transition and those found for the V66W′. The sum of the free energies of unfolding involved in the two steps is about 1.5 kcal/mol less than the value obtained for the unfolding of WT SNase,

suggesting a nonnegligible perturbation of the structure by the mutation. From the magnitudes of the free energy changes, we conclude that I is slightly closer in free energy to U than it is to N, and, interestingly, the same trend was observed in the three-state unfolding study of apomyoglobin (Barrick & Baldwin, 1993). In addition, the two transitions for apomyoglobin were found to be equally sensitive to urea, and we also find $m_{IN} \approx m_{UI} \approx 1.2$ kcal mol^{-1} M^{-1} for V66W. Comparing the sum of m_{IN} and m_{UI} values of V66W, 2.4 kcal mol^{-1} M^{-1}, with the m value of WT, 2.5 kcal mol^{-1} M^{-1}, it seems that the same total surface area is exposed upon complete unfolding of both proteins.

Another result of the global analysis for V66W is that the acid-induced unfolding is triggered by one titratable group for the α-subdomain and by two or three groups for the β-subdomain. Some of the titratable groups may be the same as for WT, but the lack of an X-ray structure of V66W precludes any identification.

ACKNOWLEDGMENT

We thank Dr. Wesley Stites, University of Arkansas, for providing us with the plasmids containing the expression system for V66W and V66W′, Cing-Yuen Wong for help in protein preparation, and Dr. Robert Woody, Colorado State University, for advice in interpreting CD spectra.

REFERENCES

Alexandrescu, A. T., & Shortle, D. (1994) *J. Mol. Biol. 242*, 527−535.
Alexandrescu, A. T., Mills, D. A., Ulrich, E. L., Chinami, M., & Markley, J. L. (1988) *Biochemistry 27*, 2158−2165.
Alonso, D. O. V., Dill, K. A., & Stigter, D. (1991) *Biopolymers 31*, 1631−1649.
Andrade, M. A., Chacon, P., Merolo, J. J., & Moran, F. (1993) *Protein Eng. 6*, 383−390.
Anfinsen, C. B. (1972) *Biochem. J. 128*, 737−749.
Aune, K. C., & Tanford, C. (1969) *Biochemistry 8*, 4579−4585.
Barrick, D., & Baldwin, R. L. (1993) *Biochemistry 32*, 3790−3796.
Beechem, J. M., Gratton, E., Ameloot, M., Knutson, J. R., & Brand, L. (1991) in *Topics in Fluorescence Spectroscopy* (Lakowicz, J. R., Ed.) Vol. 2, pp 241−305, Plenum Press, New York.
Bolen, D. W., & Santoro, M. M. (1988) *Biochemistry 27*, 8069−8074.
Bull, H. B., Breese, K., Ferguson, G. L., & Swenson, C. A. (1964) *Arch. Biochem. Biophys. 104*, 297−304.
Carra, J. H., & Privalov, P. L. (1995) *Biochemistry 34*, 2034−2041.
Carra, J. H., Anderson, E. A., & Privalov, P. L. (1994a) *Protein Sci. 3*, 944−951.
Carra, J. H., Anderson, E. A., & Privalov, P. L. (1994b) *Protein Sci. 3*, 952−959.
Carra, J. H., Anderson, E. A., & Privalov, P. L. (1994c) *Biochemistry 33*, 10842−10850.
Chang, C. T., Wu, C. C., & Yang, J. T. (1978) *Anal. Biochem. 91*, 13−31.
Chen, H. M., You, J. L., Markin, V. S., & Tsong, T. Y. (1991) *J. Mol. Biol. 220*, 771−778.
Creighton, T. E., & Shortle, D. (1994) *J. Mol. Biol. 242*, 670−682.
Eftink, M. R., Ionescu, R. M., Ramsay, G. D., Wong, C. Y., Wu, J. Q., & Maki, A. H. (1996) *Biochemistry 35*, 8084−8094.
Epstein, H. F., Schechter, A. N., Chen, R. F., & Anfinsen, C. B. (1971a) *J. Mol. Biol. 60*, 499−508.
Epstein, H. F., Schechter, A. N., & Cohen, J. S. (1971b) *Proc. Natl. Acad. Sci. U.S.A. 68*, 2042−2046.
Fink, A. L. (1995) *Annu. Rev. Biophys. Biomol. Struct. 24*, 495−522.
Fink, A. L., Calciano, L. J., Goto, Y., Nishimura, M., & Swedberg, S. A. (1993) *Protein Sci. 2*, 1155−1160.
Flanagan, J. M., Kataoka, M., Shortle, D., & Engelman, D. M. (1992) *Proc. Natl. Acad. Sci. U.S.A. 89*, 748−752.
Gittis, A. G., Stites, W. E., & Lattman, E. E. (1993) *J. Mol. Biol. 232*, 718−724.
Griko, Y. V., Gittis, A. G., Lattman, E. E., & Privalov, P. L. (1994)- *J. Mol. Biol. 243*, 93−99.
Hynes, T. R., & Fox, R. O. (1991) *Proteins: Struct., Funct., Genet. 10*, 92−105.
Jacobs, M. D., & Fox, R. O. (1994) *Proc. Natl. Acad. Sci. U.S.A. 91*, 449−453.
James, E., Wu, P. G., Stites, W., & Brand, L. (1992) *Biochemistry 31*, 10217−10225.
Johnson, C. M., & Fersht, A. R. (1995) *Biochemistry 34*, 6795−6804.
Johnson, M. L., & Fraiser, S. G. (1985) *Methods Enzymol. 117*, 301−342.
Kálmán, F., Ma, S., Fox, R. O., & Horváth, C. (1995) *J. Chromatogr., A 705*, 129−134.
Kraulis, P. (1991) *J. Appl. Crystallogr. 24*, 946−950.
Loh, S. N., & Markley, J. L. (1994) *Biochemistry 33*, 1029−1036.
Makhatadze, G. I., & Privalov, P. L. (1992) *J. Mol. Biol. 226*, 491−505.
Myers, J. K., Pace, C. N., & Scholtz, J. M. (1995) *Protein Sci. 4*, 2138−2148.
Oliveberg, M., Vuilleumier, S., & Fersht, A. R. (1994) *Biochemistry 33*, 8826−8832.
Pace, C. N. (1986) *Methods Enzymol. 131*, 226−280.
Pace, C. N., Laurents, D. V., & Thomson, J. A. (1990) *Biochemistry 29*, 2564−2572.
Pace, C. N., Laurents, D. V., & Erickson, R. E. (1992) *Biochemistry 31*, 2728−2734.
Perczel, A., Park, K., & Fasman, G. D. (1992) *Anal. Biochem. 203*, 83−93.
Ramsay, G. D., & Eftink, M. R. (1994) *Biophys. J. 31*, 516−523.
Ramsay, G. D., Ionescu, R. M., & Eftink, M. R. (1995) *Biophys. J. 69*, 701−709.
Schellman, J. A. (1978) *Biopolymers 17*, 1305−1322.
Shortle, D., & Meeker, A. K. (1986) *Proteins: Struct., Funct., Genet. 1*, 81−89.
Shortle, D., & Meeker, A. K. (1989) *Biochemistry 28*, 936−944.
Sreerama, N., & Woody, R. W. (1993) *Anal. Biochem. 209*, 32−44.
Staniforth, R. A., Burston, S. G., Smith, C. J., Jackson, G. S., Badcoe, I. G., Atkinson, T., Holbrook, J. J., Clarke, A. R. (1993) *Biochemistry 32*, 3842−3851.
Sugawara, T., Kuwajima, K., & Sugai, S. (1991) *Biochemistry 30*, 2698−2706.
Tanford, C. (1970) *Adv. Protein Chem. 24*, 2−95.
Wang, Y., & Shortle, D. (1995) *Biochemistry 34*, 15895−15905.
Xie, D., Fox, R., & Freire, E. (1994) *Protein Sci. 3*, 2175−2184.
Yang, A., & Honig, B. (1994) *J. Mol. Biol. 237*, 602−614.
Yao, M., & Bolen, D. W. (1995) *Biochemistry 34*, 3771−3781.

BI9609681